Medical Physics
The International Journal of Medical Physics Research and Practice

Rapid objective measurement of gamma camera resolution using statistical moments

Trish A. Hander, Jack L. Lancaster, David T. Kopp, John C. Lasher, Ralph Blumhardt, and Peter T. Fox

Citation: Medical Physics **24**, 327 (1997); doi: 10.1118/1.597928
View online: http://dx.doi.org/10.1118/1.597928
View Table of Contents: http://scitation.aip.org/content/aapm/journal/medphys/24/2?ver=pdfcov
Published by the American Association of Physicists in Medicine

Rapid objective measurement of gamma camera resolution using statistical moments

Trish A. Hander, Jack L. Lancaster,[a] David T. Kopp, John C. Lasher, Ralph Blumhardt, and Peter T. Fox
Department of Radiology, University of Texas Health Science Center at San Antonio, San Antonio, Texas 78284

(Received 10 June 1996; accepted for publication 5 November 1996)

An easy and rapid method for the measurement of the intrinsic spatial resolution of a gamma camera was developed. The measurement is based on the first and second statistical moments of regions of interest (ROIs) applied to bar phantom images. This leads to an estimate of the modulation transfer function (MTF) and the full-width-at-half-maximum (FWHM) of a line spread function (LSF). Bar phantom images were acquired using four large field-of-view (LFOV) gamma cameras (Scintronix, Picker, Searle, Siemens). The following factors important for routine measurement of gamma camera resolution with this method were tested: ROI placement and shape, phantom orientation, spatial sampling, and procedural consistency. A 0.2% coefficient of variation (CV) between repeat measurements of MTF was observed for a circular ROI. The CVs of less than 2% were observed for measured MTF values for bar orientations ranging from $-10°$ to $+10°$ with respect to the x and y axes of the camera acquisition matrix. A 256×256 matrix (1.6 mm pixel spacing) was judged sufficient for routine measurements, giving an estimate of the FWHM to within 0.1 mm of manufacturer-specified values (3% difference). Under simulated clinical conditions, the variation in measurements attributable to procedural effects yielded a CV of less than 2% in newer generation cameras. The moments method for determining MTF correlated well with a peak–valley method, with an average difference of 0.03 across the range of spatial frequencies tested (0.11–0.17 line pairs/mm, corresponding to 4.5–3.0 mm bars). When compared with the NEMA method for measuring intrinsic spatial resolution, the moments method was found to be within 4% of the expected FWHM. [S0094-2405(97)00702-5]

Key words: gamma camera, image evaluation, quality assurance, spatial resolution, modulation transfer function, FWHM

I. INTRODUCTION

Quality control tests on gamma cameras include daily flood and weekly bar phantom images to assess spatial uniformity, resolution, and linearity. Bar phantom resolution checks entail a visual inspection of the image to detect changes in the camera's ability to resolve the narrowest bars. At least one pattern of bars should be near the limiting resolution of the camera for adequate visual evaluation.[1,2]

A. Present methods of quantifying resolution

The present methods for objective measurement of the resolution of gamma cameras are often difficult, tedious, or require special software.[3–7] All require an accurate measurement of the line spread function from which the full-width-at-half-maximum (FWHM) and modulation transform function (MTF) can be determined.[1]

The NEMA standard for measuring the intrinsic spatial resolution from the line spread function (LSF) requires the acquisition of a digital image of a line source.[8] For this measurement a point source of Tc-99(m) is commonly used in conjunction with a slit phantom. A count profile (LSF) across the line image is generated and the FWHM is calculated. These LSFs are difficult to acquire since the suggested width of the projected line is 1 mm, requiring a special-purpose slit phantom.[7,8] Acquisition times are long because of the low geometric efficiency inherent to the method. If the slit is not positioned parallel to a row or column of the digital image matrix, the measured LSF is wider than the true value. In addition, pixel spacing must be no more than one-tenth the expected FWHM. This requires an acquisition matrix of 1024^2 for large field-of-view (LFOV) cameras unless magnification is used.

Once an accurate LSF is recorded, the MTF is readily calculated by taking the Fourier transform of the normalized LSF (nLSF):

$$\mathrm{MTF}(f)=\left|\int_{-\infty}^{+\infty}\mathrm{nLSF}(x)e^{-2\pi ifx}\,dx\right|, \tag{1}$$

where

$$\mathrm{nLSF}(x)=\frac{\mathrm{LSF}(x)}{\int_{-\infty}^{+\infty}\mathrm{LSF}(x)\,dx}.$$

The LSF measures the relative magnitude of blurring as a function of distance x from the line source. The MTF expresses the response of a system in frequency space. In the

special case where the LSF is Gaussian, the MTF is also Gaussian.[9] Likewise, the inverse transform of the MTF(f) yields the nLSF(x).

B. Theoretical basis for moments method

The moments method is a rapid objective method for assessing gamma camera intrinsic spatial resolution by calculating MTF(f_b) associated with a bar pattern of frequency, f_b. Alternately, the FWHM of the LSF(x) can be calculated. The moments method uses first- and second-order statistics taken from a bar phantom image. A similar method for deriving the MTF from statistics taken from a ROI placed on a bar image has previously been developed for computed tomography (CT) scanners.[10,11] The relationship between these statistics and the MTF(f_b) of the gamma camera is derived assuming that the bar pattern in the image is sinusoidal.

The general equation for the modulation at frequency f is calculated as

$$\mathrm{MOD}(f)=\frac{\mathrm{Peak}(f)-\mathrm{Valley}(f)}{\mathrm{Peak}(f)+\mathrm{Valley}(f)}, \tag{2}$$

where Peak(f) and Valley(f) refer to the maximum and minimum values of the sinusoidal curve of frequency, f. The MTF may be defined in terms of modulation as

$$\mathrm{MTF}(f)=\frac{\mathrm{MOD}_{\mathrm{out}}(f)}{\mathrm{MOD}_{\mathrm{in}}(f)}. \tag{3}$$

For bar phantom images, $\mathrm{MOD}_{\mathrm{in}}(f)$ is assumed to be unity because of the extreme attenuation (>99%) of low-energy gammas in the lead bars, commonly 3 mm thick. The MTF(f) therefore becomes

$$\mathrm{MTF}(f)=\mathrm{MOD}_{\mathrm{out}}(f). \tag{4}$$

Rewriting Eq. (2) by dividing both numerator and denominator by 2 and substitution into Eq. (4) will reveal the relationship between modulation and the signal's first and second moments (μ and σ^2, respectively):

$$\mathrm{MTF}(f)=\frac{[\mathrm{Peak}(f)-\mathrm{Valley}(f)]/2}{[\mathrm{Peak}(f)+\mathrm{Valley}(f)]/2}. \tag{5}$$

The numerator of Eq. (5) is the signal amplitude. For a sinusoid, the relationship between the amplitude and the root-mean-squared (rms) value is amplitude=$\sqrt{2}$ rms value. The standard deviation (σ) of a sinusoid is equal to its rms value when calculated over integral multiples of the period. Likewise, the denominator is equal to the mean value (μ) of the signal when calculated over the same range.

Therefore, the MTF in terms of the mean and standard deviation calculated over integral multiples of the period of a sinusoidal signal is

$$\mathrm{MTF}(f)=\frac{\sqrt{2}\cdot\sigma(f)}{\mu(f)}. \tag{6}$$

The spacing of the bars defines a fundamental frequency (f). The bar pattern is not a true sine curve (see Sec. IV); therefore calculating the MTF from Eq. (6) using a bar phantom image yields an approximation of the true MTF. Assuming that the MTF is Gaussian (see Sec. IV), the FWHM can be calculated directly from the image statistics (see the Appendix).

II. METHODS

Of the two statistical moments needed to measure the MTF, the variance (standard deviation squared, σ^2) is more difficult to measure accurately. The variance in counts in a bar phantom image ROI (σ^2_{ROI}) is primarily due to three sources:

(1) spatial modulation introduced by the bar phantom, σ^2_{bars};
(2) random variation in the number of counts/pixel recorded, $\sigma^2_{\mathrm{noise}}$; and
(3) variation due to spatial nonuniformity, σ^2_{nu}.

The moments method for measuring the MTF requires that the variance be due entirely to the spatial modulation by the bar phantom (source 1). Variance due to the latter two sources is undesirable and must be removed to accurately measure the MTF.

The variance from sources 2 and 3 can be estimated and subtracted from the overall variance using simple methods. It was assumed that the noise variance measured in the bar image ROI was Poisson and therefore equal to the mean value measured for the ROI ($\sigma^2_{\mathrm{noise}}=\mu_{\mathrm{ROI}}$). The variance due to spatial nonuniformity was estimated from flood images as the difference between measured variance and the estimated noise variance. Assuming the three components of the total variance are uncorrelated, the variance introduced solely by the bars is calculated as

$$\sigma^2_{\mathrm{bars}}=\sigma^2_{\mathrm{ROI}}-\mu_{\mathrm{ROI}}-\sigma^2_{\mathrm{nu}}. \tag{7}$$

The variance due to spatial nonuniformity can be neglected under certain conditions. The percent differences between MTF values calculated with and without nonuniformity variance illustrate this for the gamma cameras tested. The Scintronix camera [410 mm diameter useful FOV (UFOV[8])] had a 0.3% difference for large bars (4.5 mm) and 2% difference for small bars (3.0 mm). Likewise the Picker camera (410 mm diameter UFOV) had a 0.8% difference for large bars and 5% difference for small bars. The Searle camera (370 mm UFOV) exhibited the most sensitivity to spatial nonuniformity, resulting in 4% difference for large bars and 30% difference for small bars. For cameras with good spatial uniformity as seen in the Scintronix and Picker cameras, variance due to spatial nonuniformity effects can be neglected when evaluations are made using the larger bars. The MTF at bar frequency, f_b, is then calculated using σ^2_{bars} without the σ^2_{nu} term:

$$\mathrm{MTF}(f_b)=\frac{\sqrt{2(\sigma^2_{\mathrm{ROI}}-\mu_{\mathrm{ROI}})}}{\mu_{\mathrm{ROI}}}. \tag{8}$$

Use of the moments method is illustrated in Fig. 1 for the Picker camera. The estimated FWHM is shown (see the Appendix).

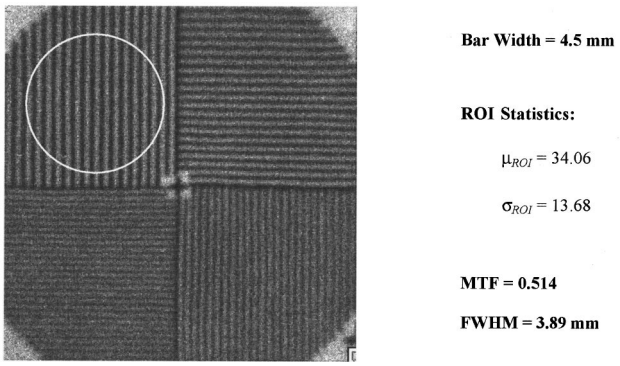

FIG. 1. Typical bar phantom image, showing a circular region of interest. The actual values obtained for the statistical measures are shown, along with the bar width and resulting MTF [from Eq. (8) in Sec. II] and FWHM [from Eq. (A8) in the Appendix]. This image was acquired using the Picker SX300 camera, with a specified FWHM of 4.1 mm.

To investigate the usefulness and accuracy of the moments method for calculating the MTF, the following were evaluated:

(i) ROI placement and shape,
(ii) phantom orientation,
(iii) spatial sampling,
(iv) procedural consistency,
(v) moments versus other methods for calculating MTF.

Bar phantom images were acquired under normal QC conditions: Tc-99m point source (small syringe) of 300–400 μCi was placed approximately five UFOV from the camera face, 20% energy window centered on the photopeak was used, correction circuits were activated, count rate was less than 20 000 cps, 2M total counts were acquired. The moments method was tested over a wide range of total counts (500 k–4M) and found to be consistent (<2% CV for the larger bar sizes). Therefore, the 2M counts normally used for QC testing is suitable for use with the moments method. For a 256^2 matrix, this corresponds to mean counts ranging from 10–78 counts/pixel in ROIs placed over the bar images. Since the expected intrinsic resolution of the cameras tested spanned a wide range (3.5–5.3 mm FWHM), two bar phantoms were used. A quadrant bar phantom consisting of 3.0–4.5 mm bars was used for the oldest camera (Searle). A quadrant bar phantom consisting of 2.0–3.5 mm bars was used in addition to the 3.0–4.5 mm phantom for the newer Picker and Scintronix cameras.

A. ROI placement and shape

From preliminary investigations, it was determined that the effect of the shape and the placement of the ROI needed to be studied. An ROI is normally positioned within the center of a bar phantom quadrant and made as large as possible while avoiding the edges. Three ROIs of different shapes were used to assess the repeat-measure reproducibility. Each ROI encompassed approximately the same number of pixels. Circular, square, and diamond-shaped ROIs were redrawn 20 consecutive times on the same quadrant in the bar phantom image (Scintronix camera). The MTF was calculated [Eq. (8)] for each repeat measurement to determine which shape yielded the most consistent MTF (smallest CV).

B. Phantom orientation

To evaluate the dependence of MTF measurements on phantom orientation, five bar phantom images were acquired on the Picker camera. The bar phantom images were obtained with the phantom successively placed at −10°, −5°, 0°, +5°, and +10° rotation. At 0° rotation, the bar phantom was carefully aligned with landmarks on the camera face that corresponded to the image matrix column direction. The angle range tested is larger than would be expected in practice. A CV was calculated to assess the variability of MTF due to orientation at each bar frequency. Because of its rotational symmetry, the circular ROI was used for this evaluation.

C. Spatial sampling

The effect of pixel size was evaluated using 128^2, 256^2, and 512^2 matrices. The Scintronix camera was used, because its specified intrinsic resolution (3.5 mm FWHM) was the smallest of the cameras evaluated. A total of 2M counts (count density of 1500 counts/cm^2) was used for each matrix size, with an additional image of 8M counts (count density of 6000 counts/cm^2) for the 512^2 image. The FWHM was estimated from the image statistics at each matrix size for comparison to the manufacturer-specified value.

D. Procedural consistency

The reproducibility of the moments method for measuring MTF was investigated using the Searle and Scintronix cameras. Ten consecutive images were acquired on each camera. Between each acquisition the phantom was repositioned and the ROIs were redrawn for each image. The intrinsic variability in the MTF measurements was evaluated by acquiring ten consecutive images without repositioning the phantom and using the same ROI for each of the images. The CVs were calculated in both instances.

E. Moments versus other methods for calculating MTF

A comparison was made between the measured MTFs using the moments method and values calculated from the manufacturer-specified FWHM assuming a Gaussian LSF [see Eq. (A5)]. The moments method for calculating the MTF was also compared to a peak–valley method. The peak–valley method to measure the MTF is based on Eqs. (2)–(4). The analysis software used (DIP Station™)[12] automatically averages across a user-selected range of profiles and reports a single average profile curve. The mean peak and valley values were calculated from this profile curve. The MTFs were calculated from Eq. (2) and compared to the MTFs obtained using the moments method [Eq. (8)]. These comparisons were made for three cameras—Scintronix, Picker, and Searle.

Finally, a NEMA slit phantom was used to measure the intrinsic resolution in the central field of view (CFOV)[8] of a Siemens DIACAM HD[3] (FOV $21'' \times 15\frac{1}{4}''$). The resulting FWHM was compared to the value obtained using the moments method. The NEMA value had been measured by the manufacturer four months prior to the measurements taken for the moments method. Data from an image of a four quadrant bar phantom (2.0–3.5 mm bars) were obtained with a total of 8M counts and a 512^2 acquisition matrix. Equation (A8) was used to calculate the FWHM using the moments method.

III. RESULTS AND CONCLUSIONS

A. ROI placement and shape

Of the three shapes tested, the circular ROI had the smallest variation in repeat measurements of the MTF ($<0.2\%$ CV vs 0.5% for the diamond-shaped ROI and 0.7% for the square ROI). The low CV for the circular ROI used for measuring MTF means that it is the least sensitive to positioning. However, the operator should make sure to avoid the edges of the quadrant. Based on these results, the circular ROI is recommended for calculating MTF.

B. Phantom orientation

The CV between MTF values measured over the $\pm 10°$ range tested was less than 2% for all bar sizes. The difference in the $-10°$ and $+10°$ angles resulted in an average change in MTF of only 0.09 across all bar frequencies tested. The $\pm 5°$ orientations reduced the average difference to 0.004. In routine testing, it is not anticipated that the orientation difference will cover an angular range of 20°, so the expected orientation effect is likely to be less than 1%. This study shows that the normal variation due to phantom placement is extremely small and therefore great care in aligning the bar phantom is not necessary when using the moments method with a circular ROI.

C. Spatial sampling

The moments method was used to calculate the FWHM for matrix sizes of 128^2, 256^2, and 512^2 on the Scintronix camera. As no matrix size greater than 256^2 was available on this camera, the 512^2 matrix was simulated by using the zoom $\times 2$ acquisition setting. The results were then compared to the 3.5 mm FWHM specified by the manufacturer. The matrix size of 128^2 caused an obvious visual degradation of the image. The 128^2 matrix gave a FWHM of 4.1 mm, the 256^2 matrix gave a FWHM of 3.4 mm, and the 512^2 matrix gave a FWHM of 3.2 mm. A 0.01 mm decrease was found between the results obtained for the 512^2 matrix size when 2M counts were acquired as compared to 8M counts. The manufacturer's FWHM value is given for the camera model, not from actual NEMA measurements on the camera that was used for this test. Although this test did not verify the absolute accuracy of the method, it was felt that the 512^2 matrix should provide the most accurate result. A matrix size of 256^2 ($\leqslant 1.6$ mm/pixel) would be sufficient for quality control purposes; however, if more accuracy is desired, a larger matrix size should be used. The smaller matrix size may be more convenient, in that not all sites have systems that can provide 512^2 matrix sizes. Using a 256^2 matrix has the added benefit of reducing the data storage requirements.

D. Procedural consistency

The CVs for ten consecutive measurements of the MTF for the Searle and Scintronix cameras are given in Fig. 2. The intrinsic variability for a camera (no phantom or ROI change) is shown by series A, while the expected variation (ROI redrawn and phantom repositioned) is shown by series B. For series A, the CV averaged across all bars was 4% for the Searle and 0.7% for the Scintronix. For series B, the CV averaged across all bars was 7.6% for the Searle and 1.2% for the Scintronix. In both series the CV increases as the bar size decreases. This can be explained by examining the relationship between the noise variance ($\sigma^2_{\text{noise}} = \mu_{\text{ROI}}$) and the total measured variance (σ^2_{ROI}). As the bar size decreases from 4.5 to 3.0 mm, the fraction of the total measured variance due to noise effects increases from 14% to 37% for the Scintronix camera. A similar increase occurs for the Searle, from 50% to 87%, resulting in more variation in the measured MTFs at the smaller bar sizes.

The procedural consistency for the Searle camera is especially troublesome for the 3.0 mm bars (16% CV for series B). The moments method is not recommended at the very low MTF values ($\leqslant 10\%$) as seen in this case. The Scintronix camera exhibited excellent procedural consistency, even for the smaller bar sizes. The measured MTF values for the Scintronix camera never dropped below 30%. If measurements are confined to the larger, more easily resolved bar patterns, the variation in repeated measures of MTF should be small ($<4\%$ for Searle and $<1\%$ for Scintronix). These measurements show that the precision of the moments method drops with increasing spatial frequency (decreasing bar size), and therefore it is recommended that the larger bars be used to minimize this effect.

E. Moments versus other methods for calculating MTF

A comparison between the MTF predicted from the camera's specifications [Eq. (A5)] and that determined by the moments method for three of the cameras studied can be made from Fig. 3. The disparity between measured and predicted MTF values increased with increasing bar frequency, with the moments method giving higher values for the smallest bars. This can be explained by examining the variance due to random noise (σ^2_{noise}) and spatial nonuniformity (σ^2_{nu}) from Eq. (7). These components of the variance are small when compared to the spatial variance (σ^2_{bars}) of the larger bars. To examine this relationship for bars of differing size, values for each of the components of variance in Eq. (7) can be compared for the large (4.5 mm) and the small (2.0 mm) bars (Scintronix camera). The large bars produced a measured variance (σ^2_{ROI}) of 278, a noise variance ($=\mu_{\text{ROI}}$) of 35, and a variance due to spatial nonuniformity effects of 3. The

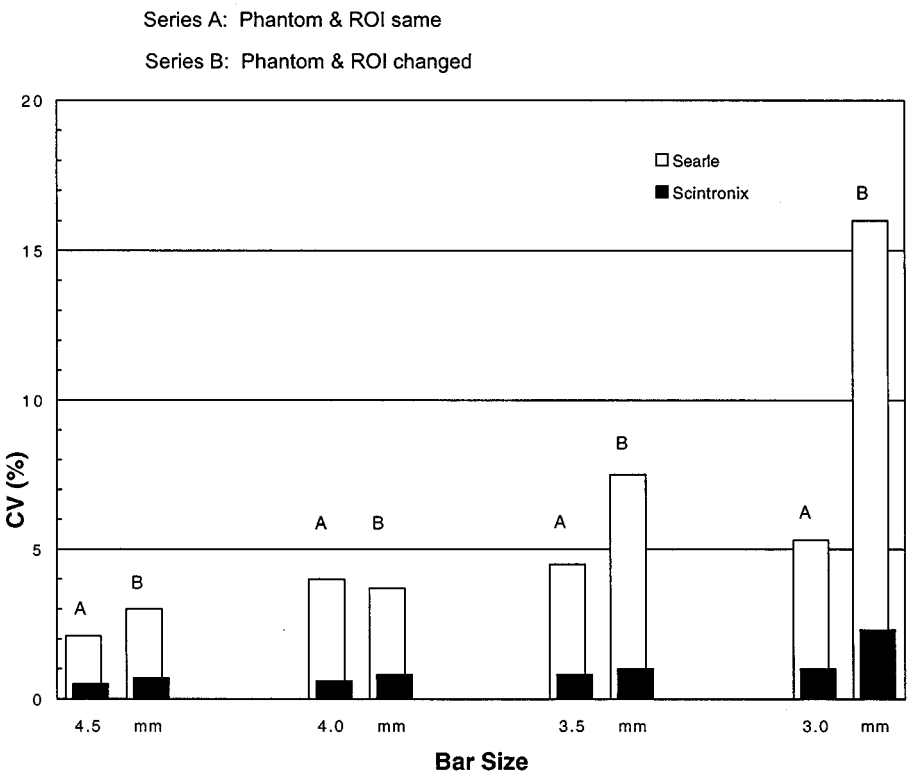

FIG. 2. Coefficient of variation in ten repeated measurements of the MTF under two different procedural conditions. In series ''A'' the bar phantom was not moved and the same ROI was used for each of the ten images. In series ''B'' the phantom was repositioned, and the ROI was redrawn between each of the ten acquisitions. Results are shown for both Searle and Scintronix cameras.

small bars produced a measured variance of 47, with similar noise and spatial nonuniformity variances. As spatial frequency increases (bar size decreases), the relative contribution of random noise and nonuniformity to the signal variance increases. The random component is accounted for as shown in Eq. (8), while the nonuniformity component is not. This reduces the accuracy of the moments method at higher spatial frequencies. However, at the large bar sizes targeted for QC use, the measured variance and MTF is high; therefore the measured and predicted MTF values agree quite well ($<$1% difference for the Searle, $<$3% difference for the Picker, and $<$5% difference for the Scintronix).

The moments method consistently produced MTFs that were larger than those obtained using the peak–valley method (Fig. 3). However, this difference was generally less than 0.03. The two main problems with the peak–valley method are (1) obtaining sufficient counts for accurately selecting peak and valley values, and (2) orienting the bars relative to the image matrix. First, to obtain sufficient counts for processing and to reduce the effects of noise, many profiles should be generated and the data averaged. This averaging produces peaks that are lower than the highest peaks and valleys that higher than the lowest valleys. The MTF values will therefore be lower than expected. Second, if great care is not taken to align the bars parallel with the image matrix rows and columns, measured modulation and estimated MTF will be low. The peak–valley method samples the data at only two points on the profile, while the moments method samples all of the data within a ROI placed on the digital bar phantom image and therefore is not as dependent on accurate localization of peaks and valleys.

Table I shows the calculated FWHM values at each bar size for the Scintronix, Picker, and Searle cameras. When the MTF is low ($<$10%), the random and spatial nonuniformity effects can cause the calculated FWHM to be smaller than expected. If the MTF is too high ($>$90%), then the sinusoidal assumption may not be correct. A MTF of approximately 50% avoids both of these problems. This can be achieved by making MTF measurements with bar sizes close to the expected FWHM since the MTF is about 40% in this case. For the newer cameras, the expected FWHM values ranged from 3.5–4.1 mm. The larger bars on the phantoms used (3.5–4.5 mm) were appropriate to use to obtain a reasonable estimate of the specified FWHM.

The NEMA protocol (using a slit phantom) yielded an average FWHM of 3.62 mm across x and y in the CFOV for the Siemens DIACAM HD[3]. The moments method predicted a 3.49 mm FWHM using the 3.5 mm bars, resulting in a 3.6% error. This resolution was measured in the x direction only, since the bar phantom design did not allow placement of the bars in the perpendicular direction. When a four-quadrant bar phantom is centered on the face of the camera, ROIs drawn in any of the quadrants will not be centered in the FOV. Rotating the bar phantom in 90° increments and combining the results from the four ROIs can produce an average measure of the FWHM across most of the FOV.

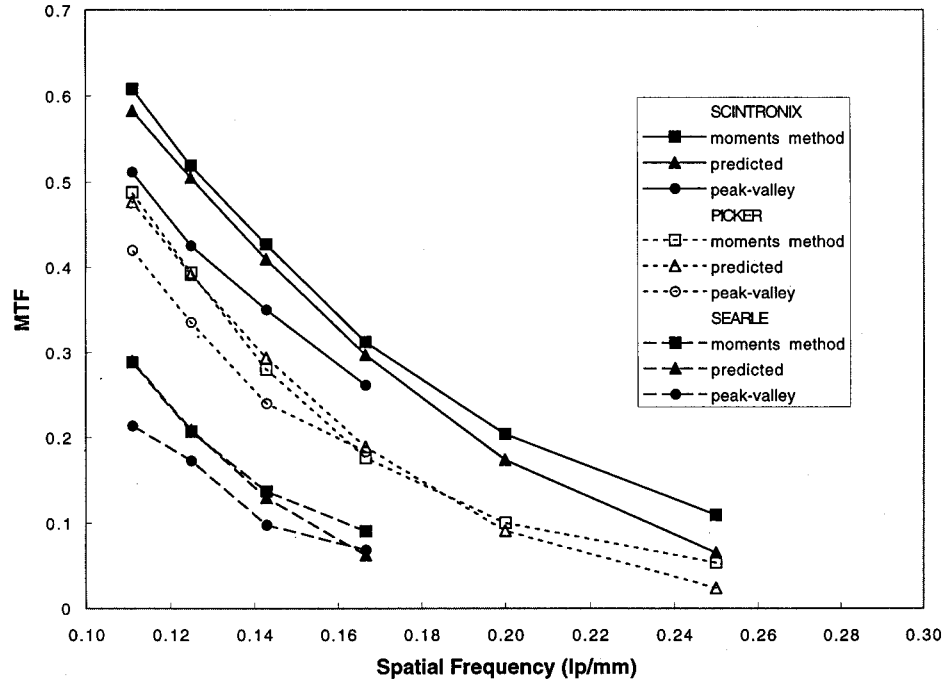

FIG. 3. The MTF for each of the bar frequencies calculated [Eq. (8) in Sec. II] using the moments method as compared to the MTF calculated [Eq. (A5) in the Appendix] using camera specifications for three cameras. More data at higher frequencies is shown for the Scintronix and the Picker cameras due to their higher resolutions (two phantoms were used). The MTF measured using a peak–valley method is also shown for the larger bar sizes [Eq. (2) in Sec. II].

Alternately, a parallel line, equal spacing (PLES) bar phantom can be used with a single large ROI centered over the FOV.

IV. DISCUSSION

The assumption regarding the sinusoidal nature of the bar phantom images can be justified by inspection of a Fourier series decomposition of the periodic square wave of a bar phantom. This decomposition shows that a square wave signal $[B(x)]$ is the superposition of a constant (signal average, B_0), a sinusoid at the bar frequency (f_b), and sinusoids at the odd harmonics ($3f_b$, $5f_b$, etc.). This is expressed as

$$B(x)=B_0+\frac{4\cdot B_0}{\pi}\left[\cos(2\pi f_b x)-\tfrac{1}{3}\cos(2\pi 3 f_b x)+\tfrac{1}{5}\cos(2\pi 5 f_b x)-\cdots\right], \quad (9)$$

where B_0 is the average of $B(x)$ over one bar period. This decomposition of a square wave is a standard approach to calculate the MTFs for a variety of imaging systems.[2] It entails the measurement of the bar pattern response at bar frequencies representing the basic frequency and its odd harmonics in order to calculate the sinusoid response or MTF at the basic frequency. The sinusoidal responses that are measured are reduced by the imaging system MTF. If the system MTF was such that harmonics contributed less than 1% to Eq. (9), we chose to neglect them. This was true for all gamma cameras and bar phantoms tested. For example, the Scintronix camera with a FWHM of 3.5 mm gave a predicted MTF of 0.582 at a bar frequency of 0.111 lp/mm (4.5 mm bars). The estimated MTF at the third harmonic was 1.3% of this value, while at the fifth harmonic it was $<0.001\%$ of this value. Under this condition, Eq. (9) is approximated with an accuracy of better than 99% using

$$B(x)=B_0+\frac{4\cdot B_0}{\pi}\left[\cos(2\pi f_b x)\right]. \quad (10)$$

This confirms that the bar pattern image is sinusoidal with a frequency equal to that of the bar pattern. For smaller bars and lower resolution cameras, the approximation of Eq. (10) is even better. Equation (10) indicates that the effective input

TABLE I. Calculated FWHMS [Eq. (A8) in the Appendix] at each bar size for three of the cameras tested. The oldest camera (Searle) was unable to resolve bar sizes smaller than 3.0 mm.

Bar size (mm)	FWHM for Searle (spec.=5.3 mm)	FWHM for Picker (spec.=4.1 mm)	FWHM for Scintronix (spec.=3.5 mm)
2.0	⋯	3.6	3.2
2.5	⋯	4.0	3.3
3.0	4.9	4.2	3.4
3.5	5.2	4.2	3.4
4.0	5.3	4.1	3.4
4.5	5.3	4.0	3.4

modulation is $4/\pi$ instead of unity as was assumed. A correction of $\pi/4$ should therefore be applied to the measured MTF to correct for this.[2] While this is theoretically correct, we have chosen not to make this correction since there is an offsetting factor that already diminishes the measured sinusoidal response due to scatter within the phantom. While the details of these offsetting factors were not studied directly, a comparison of the FWHM measured using the moments method with that measured using the NEMA standard method for the Siemens camera confirmed that not using the $\pi/4$ correction provides a good measurement of the FWHM.

The assumption that the LSF is Gaussian may not be valid, especially with respect to the ''tails'' of the curve. A comparison between the expected ratio of FWHM and full-width-at-tenth-maximum (FWTM) for a Gaussian LSF was made for two gamma cameras. Comparing the expected ratio for a Gaussian LSF (0.548) and the actual ratio for the Siemens DIACAM HD[3] camera (0.525) yielded a 4% error. The error in this ratio was found to be $<1\%$ for a Siemens 37-ZLC (390 mm circular FOV).[7] This error was assumed to be sufficiently small based on the FWHM comparisons made with the four cameras.

A basic assumption of the moments method is that the standard deviation and mean be calculated over an integral number of periods of a sinusoidal signal. It is difficult to ensure that a ROI satisfies this requirement. The error due to a partially measured period contributes less to the overall error as the size of the ROI increases. Working with various shaped ROIs and computer-generated sinusoid images, it was determined that when the diameter of a circular ROI was five to seven times the period of the sinusoid, the error due to partial sampling was acceptable. The error for circular ROIs was less than that for square and diamond-shaped ROIs. This result was verified with actual bar phantom data as reported in Sec. III. If a square ROI must be used, five to seven integral periods are recommended for each measurement of the MTF.

The moments method for measuring the MTF should be well suited for routine quality control assessment of spatial resolution in gamma cameras. Because of the low variability in repeat measurements, the moments method should prove useful for testing a camera before and after maintenance. The following steps are suggested:

(i) acquire bar phantom image [256×256 matrix (pixel size $\leqslant$1.6 mm), 2M counts, orient bars to be vertical and horizontal in the image];

(ii) process phantom image [center circular ROI within large bars, calculate μ and σ for ROI, use Eq. (8) in Sec. II to calculate MTF or Eq. (A8) in the Appendix to calculate FWHM].

Because of its simplicity and reproducibility, the procedure outlined can be used to track the week-to-week stability of the spatial resolution for all gamma cameras. The moments method may also be useful in retrospective analysis of camera resolution if bar phantom images have been stored digitally. The smallest change in FWHM that can be detected visually is about 10%.[13] Based on reproducibility measurements as shown in Fig. 2, the moments method for measuring the FWHM should be able to easily detect changes smaller than 5%. For cameras with good spatial uniformity, the moments method has repeat measure variability of less 2% for large bar sizes. This sensitivity to small changes in spatial resolution is more than adequate for the week-to-week monitoring routinely performed in a nuclear medicine clinic. For the Scintronix, Picker, and Searle cameras the FWHM was measured over an 11 week period and found to be within $\pm 5\%$ of the mean.

The moments method for rapid objective measurement of spatial resolution is quite robust. A method similar to this has been used as part of routine QC tests for CT scanners.[14] This method is insensitive to the normal variation in the positioning of the bar phantom and can be used effectively with routine bar phantom QC images. The moments method is suitable for phantoms with bar spacing on the order of the size of the expected FWHM. A four-quadrant bar phantom is not strictly necessary for the moments method. A PLES bar phantom with the appropriate bar size would be effective for this purpose, allowing for both a larger and more centered ROI to be placed on the image. Spatial calibration (pixels/mm) is not required since the moments method uses the bar size for this purpose. Because the FWHM can be readily estimated using first- and second-order statistics from a ROI, it should be easy to obtain data for a large number of systems in most nuclear medicine departments. Finally, this method may prove to be useful in other modalities that use a barlike phantom to evaluate spatial resolution, such as digital radiography.

ACKNOWLEDGMENTS

The authors would like to gratefully acknowledge the assistance of Barry Cook, Chief of Nuclear Medicine Technology at Medical Center Hospital in San Antonio, Texas for help in acquiring the data on the Searle, Picker, and Scintronix cameras; Reinout Vogt, Product Manager, Siemens Medical Systems, Inc., Nuclear Medicine Group for the NEMA measurements on the Siemens DIACAM HD[3] camera; and Brooke Army Medical Center, Department of Nuclear Medicine for help in acquiring data on the Siemens DIACAM HD[3] camera. We would also like to acknowledge the interest in our project by Dr. Ronald Walker, MD, at Radiology Consultants of Little Rock, Little Rock, Arkansas. Research support was provided by the Human Brain Project, which is funded jointly by NIMH and NIDA (P20 MH/DA 52176).

APPENDIX: CALCULATION OF FWHM

Assuming that the LSF is Gaussian, an equation for the LSF as a function of position (x) is as follows:

$$\mathrm{LSF}(x) = \frac{1}{\sigma\sqrt{2\pi}}\, e^{-x^2/2\sigma^2}, \tag{A1}$$

where σ represents the standard deviation of the LSF. The MTF can be calculated from the LSF using the Fourier transform [Eq. (1)] as

$$\mathrm{MTF}(f)=e^{-2\pi^2\sigma^2 f^2}. \tag{A2}$$

The standard deviation of a Gaussian is related to the FWHM value by

$$\sigma=\frac{\mathrm{FWHM}}{2.35}. \tag{A3}$$

The frequency of the bars f_b, in line pairs/millimeter, is related to the width of the bars according to

$$f_b=\frac{1}{2\ \mathrm{width}}. \tag{A4}$$

The MTF based on bar width and FWHM is computed by combining Eqs. (A2)–(A4):

$$\mathrm{MTF}(f_b)\approx e^{-0.894(\mathrm{FWHM}/\mathrm{width})^2}. \tag{A5}$$

Solving Eq. (A5) for the FWHM yields

$$\mathrm{FWHM}\approx 1.058\cdot\mathrm{width}\cdot\sqrt{\ln\left[\frac{1}{\mathrm{MTF}(f_b)}\right]}. \tag{A6}$$

Substituting the MTF predicted by the moments method [Eq. (6) in body of paper] into Eq. (A6), a more fundamental equation for the FWHM is obtained.

$$\mathrm{FWHM}\approx 1.058\cdot\mathrm{width}\cdot\sqrt{\ln\left[\frac{\mu(f_b)}{\sqrt{2}\cdot\sigma(f_b)}\right]}. \tag{A7}$$

To remove the effects of random noise, the mean value given by the bar phantom ROI was subtracted from the square of the standard deviation. Therefore the final expression for FWHM is

$$\mathrm{FWHM}\approx 1.058\cdot\mathrm{width}\cdot\sqrt{\ln\left(\frac{\mu(f_b)}{\sqrt{2[\sigma^2(f_b)-\mu(f_b)]}}\right)}. \tag{A8}$$

The FWHM of the LSF can be estimated using Eq. (A8) from bar phantom images, given the width of the bars in the phantom as well as the mean (μ) and standard deviation (σ) calculated for a ROI in a bar quadrant.

[a]Address for correspondence: University of Texas Health Science Center at San Antonio, 7703 Floyd Curl Drive, San Antonio TX 78284-6240. Electronic mail: jlancaster@uthscsa.edu

[1]P. H. Murphy, ''Acceptance testing and quality control of gamma cameras, including SPECT,'' J. Nucl. Med. **28**, 1221–1227 (1987).
[2]J. W. Coltman, ''The specification of imaging properties by response to a sine wave input,'' J. Opt. Soc. Am. **44**, 468–471 (1954).
[3]H. Norwood, A. Walker, A. Parkin, and A. Hall, ''Use of a personal computer to measure gamma camera spatial resolution,'' Br. J. Rad. **61**, 237–239 (1988).
[4]J. Lancaster, D. Kopp, J. Lasher, and R. Blumhardt, ''Practical gamma camera quality control with a four-point phantom,'' J. Nucl. Med. **26**, 300–307 (1985).
[5]U. Raff, V. Spitzer, and W. Hendee, ''Practicality of NEMA performance measurements for user-based acceptance testing and routine quality assurance,'' J. Nucl. Med. **25**, 679–687 (1984).
[6]B. Hasegawa, D. Kirch, M. Lefree, R. Vogel, P. Steele, and W. Hendee, ''Quality control of scintillation cameras using a minicomputer,'' J. Nucl. Med. **22**, 1075–1080 (1981).
[7]W. A. Waddington, G. A. Clarke, K. J. Barnes, G. J. Gillen, A. T. Elliot, and M. D. Short, ''A reappraisal of current methods for the assessment of planar gamma camera performance,'' Nucl. Med. Comm. **16**, 186–195 (1995).
[8]''Performance measurements of scintillation cameras,'' Standards Publication No. NU1, Washington, DC: National Electrical Manufacturers Association (1986).
[9]R. Bracewell, *The Fourier Transform and Its Application* (McGraw-Hill, New York, 1986), p. 54.
[10]R. T. Droege and R. L. Morin, ''A practical method to measure the MTF of CT scanners,'' Med. Phys. **9**, 758–760 (1982).
[11]R. T. Droege, ''A practical method to routinely monitor resolution in digital images,'' Med. Phys. **10**, 337–343 (1983).
[12]''DIPS (*D*igital *I*mage *P*rocessing *S*tation),'' Hayden Image Processing Group, P.O. Box 654, Boulder, CO 80306-0654.
[13]B. Kasal, P. F. Sharp, and P. P. Dendy, ''Relationship between objective and subjective assessment of gamma camera image sharpness,'' Phys. Med. Biol. **28**, 1127–1134 (1983).
[14]GE Medical Systems CT HiSpeed Advantage, Technical Reference Manual—Quality Assurance Section, GE Medical Systems Americas, P.O. Box 414, Milwaukee, WI 53201 (1993).